CIÊNCIA e NATURA

ISSN 2179-460X

OPEN ACCESS

Ci. e Nat., Santa Maria, v. 48, e91903, 2026• https://doi.org/10.5902/2179460X91903
Submitted: 06/05/2025 • Approved: 29/10/2025 • Published: 23/07/2026

Mathematics

Alifanov's Iterative Regularization Method for the Poisson Source Term on Spherical Surfaces using Icosahedral Meshes

Método de regularização iterativa de Alifanov para função de termo de fonte de Poisson em superfícies esféricas com malha icosaedral

Fábio Freitas Ferreira [I], **Francisco Duarte Moura Neto** [II]

[I]Universidade Federal Fluminense, RJ, Brazil
[II]Universidade do Estado do Rio de Janeiro, RJ, Brazil

ABSTRACT

In the Poisson problem, given measurements at specific points on the sphere, the goal is to determine the source term that maintains a stationary distribution. The forward problem was solved using a dual icosahedral mesh, chosen for its quasi-regularity, which is beneficial for a wide range of applications. The objective of this work is to solve the inverse problem in order to obtain the source term of the Poisson equation defined on the sphere. To solve the inverse problem, Alifanov's iterative regularization method is applied. The inverse problem solution was validated using synthetic experimental data, which successfully recovered the source term. Perturbations of up to 10% preserved the overall behavior of the source term, albeit with amplified values.

Keywords: Poisson equation; Icosahedral mesh; Inverse problem; Alifanov; Source term

RESUMO

No problema de Poisson, dadas medições em pontos específicos da esfera, o objetivo é determinar o termo fonte que mantém uma distribuição estacionária. O problema direto foi resolvido utilizando uma malha icosaédrica dual, escolhida por sua quase-regularidade, que é benéfica para uma ampla gama de aplicações. O objetivo deste trabalho é resolver o problema inverso para obter o termo fonte da equação de Poisson definida na esfera. Para resolver o problema inverso, o método de regularização iterativa de Alifanov foi aplicado. A solução do problema inverso foi validada utilizando dados experimentais sintéticos, que recuperaram com sucesso o termo fonte. Perturbações de até 10% preservaram o comportamento geral do termo fonte, embora com valores amplificados.

Palavras-chave: Equação de Poisson; Malha icosaedral; Problema inverso; Alifanov; Termo fonte

1 INTRODUCTION

The determination of the source term of the Poisson equation on the surface of the sphere was addressed by Ferreira (2008). This type of problem is classified as a Type III inverse problem, according to Moura Neto & Silva Neto (2012). In the Poisson problem, given temperature measurements at several points on the sphere, one seeks to determine the thermal source that maintains a stationary temperature distribution.

To solve the Poisson problem on the sphere, an icosahedral mesh and its corresponding dual mesh were employed (Moura Neto & Ferreira, 2006,0,0). The icosahedral mesh provides a nearly regular point distribution. Other types of spherical meshes exist. Meshes based on Mercator projection, for instance, accumulate a high density of points near the North and South poles, while showing a sparse distribution along the equator. The icosahedral mesh and its respective dual mesh exhibit Voronoi–Delaunay characteristics (Augebaum & Peskin, 1985), and are constructed from an arbitrary Delaunay triangulation of the sphere, developed by Renka (1984a,8,8,9). Chukkapalli et al. (1999) proposed a scheme for generating unstructured meshes on the sphere, for example using spirals, with applications to parallel computing. Sibson (1978) presented rules for locally equiangular triangulations. Teanby (2006) introduced a method based on an icosahedral mesh to globally categorize remotely sensed distributed data. Tomita et al. (2002) proposed an optimized modified icosahedral mesh. Lanser et al. (2000) used stereographic coordinates on the sphere to solve the shallow water equations.

However, the quasi-regularity offered by the chosen mesh is not attainable with these alternative approaches. Therefore, a mesh was constructed based on an icosahedron, known as an icosahedral mesh, as presented by Baumgardner & Friderickson (1985), along with a sequence of icosahedral meshes with dyadic refinement and their corresponding dual meshes on the sphere. Since dyadic refinement is performed by determining the midpoint of each edge and projecting it onto the sphere, the quasi-regularity is preserved (Baumgardner & Friderickson, 1985; Moura Neto & Ferreira, 2006,0,0).

Tulovsky & Papiz (2001) derived a simple asymptotic formula for the fundamental solution of the heat equation on the sphere for small values of the evolution parameter. This complements the formula for the fundamental solution in terms of Legendre polynomials, which is more efficient for relatively large values of the evolution parameter. Nicholson & Shelton (2002) computed the Hartree potential using a direct method to solve the Poisson equation for expressed charge densities. Stuhne & Peltier (1996,9) and Karpik & Peltier (1991) employed icosahedral meshes to obtain a discretization of the shallow water equations on the sphere. Heikes and Randall Heikes & Randall (1995a,9) presented a discretization of the shallow water equations on the sphere using an icosahedral mesh and its modified dual mesh, aiming to improve the numerical solution. This proposed discretization is based on the work of Nicolaides (1992), who solved divergence and rotational problems using dual meshes on the sphere, as well as the work of Gonçalves & Moura Neto (2005) and Douglas Jr. et al. (1993), who conducted an in-depth discussion of the discretization of equilibrium equations in the plane using dual meshes. In this work, the algorithm developed by Moura Neto & Ferreira (2006,0,0) was used to solve the Poisson equation using dual meshes.

Siewert (1994) solved the inverse radiative transfer problem for a sphere. Wallis & McEwen (2017) applied inverse problems to reconstruct sparse images on the sphere. Sjöberg (2012) applied Tikhonov regularization to obtain solutions to linear inverse problems on the sphere. The objective of this work is to determine the source term of the Poisson equation by solving an inverse problem. To solve the inverse problem, we applied Alifanov's iterative regularization method (Alifanov, 1974; Alifanov & Mikhailov, 1978; Moura Neto & Silva Neto, 2012), for solving the inverse problem defined on the sphere. The conjugate gradient method was employed to minimize the squared residual functional (Moura Neto & Silva Neto, 2012).

2 THE POISSON PROBLEM ON THE SPHERE

The Poisson problem on the sphere (S^2) consists of, given a source term f, determining a function u, both defined on S^2, such that the following partial differential equation is satisfied

$$-\Delta_S u(x) = f(x), \quad x \in S^2 , \tag{1}$$

where Δ_S is the Laplacian operator on the sphere.

The Poisson problem in terms of first-order operators is given by

$$\mathsf{div}_S \overrightarrow{v}(x) = f(x) \ , \quad x \in S^2 \ , \tag{2}$$

$$-\nabla_S u(x) = \overrightarrow{v} \ , \quad x \in S^2 \ . \tag{3}$$

where $\overrightarrow{v}$ and u, called flux and potential, respectively, are unknowns and f is the source and/or sink of the problem.

The problem does not have a unique solution because if the pair $(u, \overrightarrow{v})$ is a solution of the system of equations (2-3), then $(u + c, \overrightarrow{v})$, where c is an arbitrary constant, will also be a solution. We choose a unique solution by imposing that $\int_{S^2} u \, dS = 0$.

Furthermore, by the divergence theorem of vector fields defined on surfaces,

$$\int_{S^2} f(x) \ dS(x) = \int_{S^2} \mathsf{div}_S \overrightarrow{v} \, dS(x) = \int_{\partial S^2 = \emptyset} \overrightarrow{v} \cdot \hat{n} \, dS(x) = 0 \tag{4}$$

since the boundary of S^2 is empty. It follows that a necessary condition for the system of equations (2-3) to have a solution is that the source has a zero mean over the sphere, $\int_{S^2} f(x) \ dS(x) = 0$.

To solve the system of Eqs. (2-3), an icosahedral mesh and its corresponding dual mesh are employed, see Figure 1. The icosahedral mesh is constructed from a regular icosahedron inscribed in the sphere and is refined through dyadic subdivisions, which are obtained by connecting the midpoints of the edges with geodesic arcs. The dual mesh is generated from the circumcenters of the triangles of the icosahedral mesh, resulting in pentagonal and hexagonal polygons distributed across the surface. Figure 2(c) illustrates the relationship between the dual and icosahedral meshes. The potential, $u(x)$, is defined at the vertices of the icosahedral mesh, while the flux $\overrightarrow{v}$ is calculated at the edges of the dual mesh.

Figure 1 – Level 1 mesh - relationship between the icosahedral meshes and their respective dual meshes.

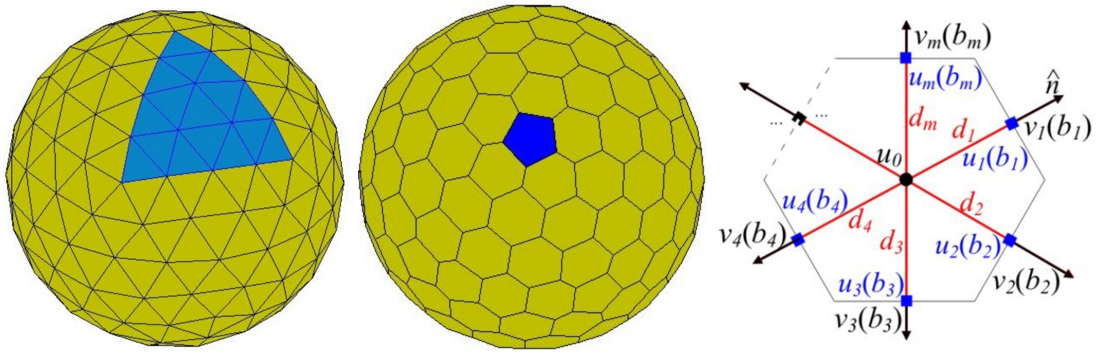

(a) Icosahedral mesh (b) Dual mesh (c) Relationship between meshes

The solution to the Poisson problem on the sphere was presented in the works of Moura Neto & Ferreira (2006,0,0).

3 STATIONARY SOURCE ESTIMATION PROBLEM ON THE SPHERE

This section presents the algorithm for estimating heat sources with spatial dependence, from simulated experimental measurements of the temperature distribution on the sphere, using the Alifanov iterated regularization method, (Alifanov & Mikhailov, 1978; Moura Neto & Silva Neto, 2012), to solve the inverse Poisson problem defined on the sphere.

Although the residual functional minimization is performed using the conjugate gradient method, the overall formulation retains the fundamental characteristics of Alifanov's iterative regularization method (1974). Regularization is incorporated implicitly into the iterative process by controlling the step size and the stopping criterion based on the discrepancy principle. Thus, the use of the conjugate gradient method is a numerical strategy to accelerate convergence without altering the regularizing nature of Alifanov's method. In other words, the algorithm used here constitutes a variational implementation of Alifanov's method, in which the source term estimates are iteratively updated to ensure stability against noise and the ill-posed nature of the inverse problem (Moura Neto et al., 2002).

3.1 Poisson problem and the inverse problem formulation

Consider the Poisson problem given in eq. (1). Denote the solution by $u[f]$, making explicit its dependence on the source term.

The inverse problem associated with the Poisson equation consists of estimating the source, knowing the problem formulation and the experimental measurements. That is, one aimed to determine $f(x)$, $x \in S^2$, from experimental measurements, u_m, of the temperature at the prescribed positions $x_m \in S^2$ with $m = 1, \ldots, M$. Note that x_m, $m = 1, \ldots, M$ represents the position of the temperature sensors.

The inverse problem was solved through optimization, minimizing the quadratic functional of the residues

$$J[f] = \frac{1}{2} \sum_{m=1}^{M} \{u[f](x_m) - u_m\}^2 . \tag{5}$$

Here f is the function to be estimated, $f : S^2 \to I\!R$, u_m is the measured quantity, and $u[f]$ is the calculated quantity due to the source f, $u[f] : S^2 \to I\!R$, that is, $u[f]$ is the solution of the equation (1) with f given. Note that, $u[f](x_m)$ and u_m, with $m = 1, \ldots, M$, are defined at vertices of the icosahedral mesh, and $M \leq \mathcal{V}_n$, where $\mathcal{V}_n$ is the number of vertices of the mesh and n is its refinement level (Moura Neto & Ferreira, 2006). In this work we adopted $M = \mathcal{V}_n$. However, strategies for positioning the sensors on different parts of the sphere can be adopted, such as placing them only at the poles, for example.

3.2 Minimization procedure - conjugate gradient

To estimate the source f, the conjugate gradient method was used, which directly considers the functional minimization problem, constructing a minimizing sequence. Then let

$$f^{k+1} = f^k - \beta P^k, \tag{6}$$

where $k = 0, 1, 2, \ldots$, is the iteration count, β specifies the step size to be taken in the search direction, P_k, where

$$P^k = J'_{f^k} + \gamma^k P^{k-1}, \tag{7}$$

with $\gamma^0 = 0$. Here γ^k is the so-called conjugate coefficient, and J'_{f^k} is the gradient of the functional J at the point (function) f. It is relevant to note that both the gradient, J'_f, and the direction of the search step are scalar functions defined on S^2.

The search step size, β, is determined by minimizing the functional $J[f^{k+1}] = J[f^k - \gamma P^k]$ with respect to γ, that is,

$$J[f^k - \beta P^k] = \min_{\gamma}[f^k - \gamma P^k] = \min_{\gamma} \frac{1}{2} \sum_{m=1}^{M} \left\{ u\left[f^k - \gamma P^k\right](x_m) - u_m \right\}^2 . \tag{8}$$

Therefore, β is given by

$$\beta = \frac{\sum_{m=1}^{M} \left\{ u\left[f^k\right](x_m) - u_m \right\} \Delta u\left[P^k\right](x_m)}{\sum_{m=1}^{M} \left\{ \Delta u\left[P^k\right](x_m) \right\}^2} , \tag{9}$$

where $\Delta u = \Delta u[P]$ represents the solution of the sensitivity problem with input data P.

The conjugate coefficient, γ^k, can be chosen by setting

$$\gamma^k = \int_{S^2} \left[J'_{f^k}(x)\right]^2 dS(x) \Big/ \int_{S^2} \left[J'_{f^{k-1}}(x)\right]^2 dS(x) , \tag{10}$$

where the gradient, J'_f, is obtained by solving the adjoint equation.

3.3 Sensitivity problem

A problem that varies as a function of a given f can be associated with the sensitivity problem. By introducing a disturbance, Δf, in the given (source term), $f \to f + \Delta f$, a variation in the solution of the problem (unknown function) is obtained, $u \to u + \Delta u$. The sensitivity problem is, by definition, the problem that Δu satisfies.

Thus, the first equation given in (1) for the source $f + \Delta f$ can be rewritten as

$$-\Delta_S[u(x) + \Delta u(x)] = f(x) + \Delta f(x), x \in S^2. \tag{11}$$

Subtracting equation (1) from equation (11), we obtain the equation that Δu satisfies the sensitivity problem, given by

$$-\Delta_S[\Delta u(x)] = \Delta f(x), x \in S^2. \tag{12}$$

The dependence of $\Delta u(x)$ on the source Δf is written as $\Delta u[\Delta f](x)$. It can be seen that, in this case, the sensitivity problem is identical to the original problem, first equation in (1), varying only the source term.

3.4 Adjoint problem

To obtain the adjoint problem of a linear problem, it is convenient to set up the Lagrangian function. Let then be

$$\begin{aligned} \mathcal{L}[f] &= J[f] + \int_{S^2} \lambda(x) \left[\Delta_S u(x) + f(x)\right] dS(x) \\ &= \frac{1}{2} \sum_{m=1}^{M} \left\{u[f](x_m) - u_m\right\}^2 + \int_{S^2} \lambda(x) \left[\Delta_S u(x) + f(x)\right] dS(x) \end{aligned} \tag{13}$$

where $\lambda(x)$ is called the adjoint function (or Lagrange multiplier).

The objective is to determine the derivative of $\mathcal{L}$ at f, $d\mathcal{L}_f$. The value of $\mathcal{L}$ on the perturbed data is then calculated,

$$\begin{aligned} \mathcal{L}\left[f + \Delta f\right] &= \frac{1}{2} \sum_{m=1}^{M} \left\{u\left[f\right]\left(x_m\right) + \Delta u\left[\Delta f\right]\left(x_m\right) - u_m\right\}^2 \\ &+ \int_{S^2} \lambda(x) \left\{\Delta_S \left[u(x) + \Delta u(x)\right] + f(x) + \Delta f(x)\right\} dS(x) \end{aligned} \tag{14}$$

Rearranging you have to

$$\begin{aligned} \mathcal{L}\left[f + \Delta f\right] &= \frac{1}{2} \sum_{m=1}^{M} \left\{u\left[f\right]\left(x_m\right) - u_m\right\}^2 + \int_{S^2} \lambda\left(x\right) \left[\Delta_S u(x) + f(x)\right] dS(x) \\ &+ \sum_{m=1}^{M} \left\{u[f](x_m) - u_m\right\} \Delta u[\Delta f](x_m) + \int_{S^2} \lambda(x) \left[\Delta_S(\Delta u(x)) \right. \\ &+ \left. \Delta f(x)\right] dS(x) + \frac{1}{2} \sum_{m=1}^{M} \left\{\Delta u[\Delta f](x_m)\right\}^2 \end{aligned} . \tag{15}$$

The sum of the first two terms on the right-hand side of equation (15) corresponds to $\mathcal{L}[f]$, given in equation (13). Thus,

$$\begin{aligned} \mathcal{L}\left[f + \Delta f\right] - \mathcal{L}\left[f\right] &= \sum_{m=1}^{M} \left\{u\left[f\right]\left(x_m\right) - u_m\right\} \Delta u\left[\Delta f\right]\left(x_m\right) \\ &\quad + \int_{S^2} \lambda(x) \left[\Delta_S(\Delta u(x)) + \Delta f(x)\right] dS(x) \\ &\quad + \frac{1}{2} \sum_{m=1}^{M} \left\{\Delta u[\Delta f](x_m)\right\}^2 . \end{aligned} \tag{16}$$

The derivative of $\mathcal{L}$ at f, applied to Δf, $d\mathcal{L}_f[\Delta f]$, is obtained from equation (16) by disregarding the second-order terms in Δf (only the last term on the right-hand side of equation (16). Therefore,

$$\begin{aligned} d\mathcal{L}_f\left[\Delta f\right] &= \textstyle\sum_{m=1}^{M}\left\{u[f](x_m)-u_m\right\}\Delta u[\Delta f](x_m) \\ &+ \textstyle\int_{S^2}\lambda(x)\Delta_S(\Delta u(x))dS(x)+\int_{S^2}\lambda(x)\Delta f(x)dS(x). \end{aligned} \tag{17}$$

The inner product and the commutation property of the Laplacian are used in the inner product. Therefore, we have

$$\int_{S^2}\lambda(x)\Delta_S(\Delta u(x))dS(x)=\langle\lambda,\Delta_S(\Delta u)\rangle=\langle\Delta_S\lambda,\Delta u\rangle=\int_{S^2}\left[\Delta_S\lambda(x)\right]\Delta u(x)dS(x) \tag{18}$$

wherein,

$$\begin{aligned} d\mathcal{L}_f[\delta f] &= \textstyle\sum_{m=1}^{M}\left\{u[f](x_m)-u_m\right\}\Delta u[\Delta f](x_m) \\ &+ \textstyle\int_{S^2}\left[\Delta_S\lambda(x)\right]\Delta u(x)dS(x)+\int_{S^2}\lambda(x)\Delta f(x)dS(x). \end{aligned} \tag{19}$$

Note that

$$\begin{aligned} &\textstyle\sum_{m=1}^{M}\left\{u[f](x_m)-u_m\right\}\Delta u[\Delta f](x_m) \\ &= \textstyle\int_{S^2}\left\{\sum_{m=1}^{M}\left[u[f](x_m)-u_m\right]\Delta u[\Delta f](x_m)\delta_{x_m}(x)\right\}dS(x) \end{aligned}, \tag{20}$$

where $\delta=\delta_{x_m}(x)$ represents the Dirac function δ centered at x_m.

Thus, we have

$$\begin{aligned} d\mathcal{L}_f\left[\Delta f\right] &= \textstyle\int_{S^2}\left\{\sum_{m=1}^{M}\left[u\left[f\right](x_m)-u_m\right]\delta_{x_m}(x)\right. \\ &\quad \left.+\Delta_S\lambda(x)\right\}\Delta u\left[\Delta f\right](x)dS(x)+\int_{S^2}\lambda(x)\Delta f(x)dS(x). \end{aligned} \tag{21}$$

A function λ is chosen so as to cancel the first term on the right-hand side of the equation (21), for any Δf or for any Δu. It is then sufficient that λ satisfies the following equation:

$$-\Delta_S\lambda(x)=\sum_{m=1}^{M}\left\{u\left[f\right](x_m)-u_m\right\}\delta_{x_m}(x), x\in S^2. \tag{22}$$

This way, $d\mathcal{L}_f[\Delta f] = \int_{S^2}\lambda(x)\Delta f(x)dS(x)$. Writing in inner product notation, $\int_{S^2}\lambda(x)\Delta f(x)dS(x)=\langle\lambda,\Delta f\rangle$, we have to $d\mathcal{L}_f[\Delta f]=\langle\lambda,\Delta f\rangle$.

But, the gradient, $\mathcal{L}'_f$, by definition, is the function that represents the derivative with respect to the inner product, that is, $d\mathcal{L}_f[\Delta f]=\langle\mathcal{L}'_f,\Delta f\rangle$ where do you get $\mathcal{L}'_f=\lambda$.

According to the first equation given in (1), the term that multiplies λ in $\mathcal{L}$ in the equation (13) is null, which means that $J[f] = \mathcal{L}[f, \lambda]$. Therefore, the derivatives are equal, $dJ_f = d\mathcal{L}_f$, and the gradients are also equal, $J'_f = \mathcal{L}'_f$. Hence, we conclude that

$$J'_f = \lambda(x), \tag{23}$$

is the solution of the adjoint problem, and the equation (22) is the adjoint problem. The adjoint problem, in this case, is of the same nature as the original problem, first equation in (1), and the source term reflects the form of the functional J, equation (5).

3.5 Search step size

To obtain the search step size of the iterative algorithm for this specific problem, the critical point is calculated

$$J[f - \gamma P] = \frac{1}{2} \sum_{m=1}^{M} \left\{ u[f](x_m) - u_m - \gamma \Delta u[P](x_m) \right\}^2 . \tag{24}$$

Then, the derivative of the functional with respect to γ is calculated, given by

$$\frac{d}{d\gamma} J[f - \gamma P] = \sum_{m=1}^{M} \left\{ u[f](x_m) - u_m - \gamma \Delta u[P](x_m) \right\} \Delta u[P](x_m). \tag{25}$$

Replacing in the previous expression of the derivative, γ by β, f by f^k and P by P^k, and writing the corresponding critical point equation, we have that

$$\sum_{m=1}^{M} \left\{ u\left[f^k\right](x_m) - u_m - \beta \Delta u\left[P^k\right](x_m) \right\} \Delta u\left[P^k\right](x_m) = 0, \tag{26}$$

that is,

$$\sum_{m=1}^{M} \left\{ u[f^k](x_m) - u_m \right\} \Delta u[P^k](x_m) - \beta \sum_{m=1}^{M} \left\{ \Delta u[P^k](x_m) \right\}^2 = 0. \tag{27}$$

Solving the critical point equation with respect to β we obtain

$$\beta = \frac{\sum_{m=1}^{M} \left\{ u[f^k](x_m) - u_m \right\} \Delta u[P^k](x_m)}{\sum_{m=1}^{M} \left\{ \Delta u[P^k](x_m) \right\}^2} \tag{28}$$

3.6 Iterative algorithm

The iterative algorithm to obtain the desired solution is given by:

STEP 1: Let $k = 0$ and initialize f^0 with an initial estimate.

STEP 2: Solve the direct problem, with the source term f^k, $u[f^k]$, due to the estimate f^k (eq. (1)).

STEP 3: Knowing $u[f^k]$ that was calculated, and the experimental measurements u_m, $m = 1, \ldots, M$, determine $J'_{f^k} = \lambda$ through the adjoint problem (eq. (23)).

STEP 4: Calculate the conjugate coefficient, γ^k (eq. (10)).

STEP 5: Calculate the search direction, P^k (eq. (7)).

STEP 6: Let $\Delta f^k = P^k$ and solve the sensitivity problem by obtaining $\Delta u[P^k]$ (eq. (12)).

STEP 7: Calculate the search step size, β (eq. (28)).

STEP 8: Calculate the new estimate f^{k+1} (eq. (31)).

STEP 9: Stop if the stopping criterion is met, ie, $\max_{i=1:\mathcal{V}_n} |f_i^{k+1} - f_i^k| < \epsilon$, where ϵ is a predefined constant. Otherwise, set $k = k + 1$ and return to step 2.

4 RESULTS

The algorithm was implemented in Scilab. Numerical simulations were performed on a Dell G3 notebook equipped with an Intel(R) Core(TM) i7-10750H processor (base frequency of 2.60 GHz), 16 GB of RAM, and a 64-bit operating system based on x64 architecture.

To compare and validate the numerical solution obtained through the iterative algorithm, a particular analytical solution to the problem is used, Figure 2, given by

$$u(\theta, \varphi) = \sin^3 \varphi \cos \theta, \quad 0 \leq \theta < 2\pi, \quad 0 \leq \varphi \leq \pi, \tag{29}$$

Since the problem is defined on a sphere, the function is defined in spherical coordinates. The Laplacian operator in spherical coordinates on a sphere of radius 1 is given by

$$\Delta_s u = \frac{1}{\sin\varphi}\frac{\partial}{\partial\varphi}(\sin\varphi\frac{\partial u}{\partial\varphi}) + \frac{1}{\sin^2\varphi}\frac{\partial^2 u}{\partial\theta^2} \tag{30}$$

The source term of the Poisson equation (solution of the inverse problem), equation (1), is obtained by substituting u given in (29) into equation (1).

Therefore, the first term of equation (30) is given by

$$\frac{1}{\sin\varphi}\frac{\partial}{\partial\varphi}(\sin\varphi\frac{\partial f}{\partial\varphi}) = 3\cos\theta\sin\varphi(3\cos^2\varphi - \sin^2\varphi).$$

The second term is

$$\frac{1}{\sin^2\varphi}\frac{\partial^2 f}{\partial\theta^2} = -\sin\varphi\cos\theta.$$

Adding both terms, and developing algebraically, we obtain

$$\Delta f = 4\sin\varphi\cos\theta(3\cos^2\varphi - 1).$$

According to equation (1), $f = -\Delta_s u$. Then, the source term is given by

$$f(\theta,\varphi) = 4\sin\varphi\cos\theta(1 - 3\cos^2\varphi), \quad 0 \le \theta < 2\pi, \quad 0 \le \varphi \le \pi. \tag{31}$$

To validate the solution of the inverse problem, $f(\varphi,\theta)$, experimental measurements (u_m) are required. By using the analytical solution of the direct problem $u(\varphi,\theta)$ as input, it is expected that the source term $f(\varphi,\theta)$ will be recovered. However, real experimental measurements contain noise, collection errors, and other artifacts. To simulate these imperfections, a disturbance is introduced into the analytical solution of the direct problem to generate synthetic experimental data. The objective is to verify how these perturbations in the experimental measurements influence the solution of the inverse problem.

The experimental measurements, u_m, are synthetic and are obtained from the analytical solution of the direct problem, given by equation (29). This solution is randomly perturbed - positively or negatively - by means of a command implemented in the programming language used, respecting a previously defined percentage of perturbation on the value of the function at the point. This generates the synthetic experimental measurements used in subsequent analyses.

Figure 2 – Graphical representation of the analytical solution, eq. 29, using a color scale on the sphere.

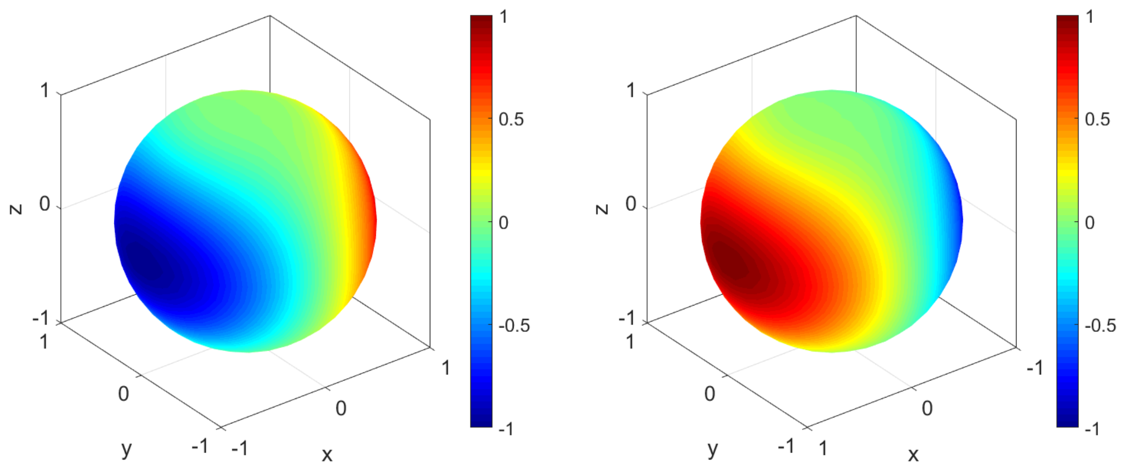

(a) Analytical solution (b) Analytical solution rotated by 180^0

The direct problem was solved by means of an iterative algorithm (Moura Neto & Ferreira, 2006,0,0), in which the stopping criterion was 10^{-5}. The direct problem, solved on the dual mesh, converges to the solution (Ferreira, 2008). A stricter stopping criterion for the direct problem leads to faster iterations in the inverse problem but may result in longer overall convergence times. For the inverse problem the stopping criterion was set at 10^{-3}. For the meshes of levels 0 and 1 the algorithm converged quickly as can be seen in Table 1. For the mesh of level 2, despite the large number of iterations, $2{,}718$, the execution time of the algorithm was small, 344.38 seconds. However, the level 3 mesh required a large computational effort, with $17{,}530$ iterations and approximately 9.2 hours of algorithm execution. The level 0 mesh has 12 points, the level 3 mesh has 642 points (Ferreira, 2008), making one iteration of the algorithm take longer. At this point, the need to use a larger stopping criterion for the direct problem is evaluated.

Another point observed in Figure 3 was that the algorithm converged to the stopping criterion of 10^{-2} with few iterations. In Figure 4(b), this convergence can be observed from iteration $1{,}000$. However, in Figure 4(a), with only 116 iterations, it is already possible to observe the satisfaction of the stopping criterion in 5×10^{-2}.

Figure 3 – Evaluation of the stopping criterion over iterations.

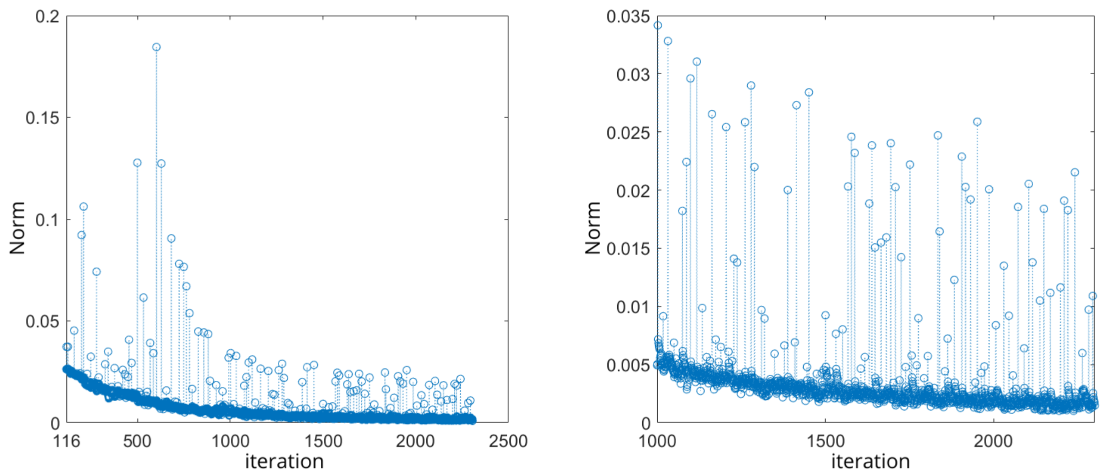

(a) Malha 0 (b) Malha 1

In this first analysis, we performed the simulation using the meshes of levels 0, 1 and 2, Table 1. For this, we use the metric N_∞ defined as $N_\infty = \max_{i=1:\mathcal{V}_n} |f_i^{\text{ip}} - f_i^{\text{ana}}|$, that is, the maximum absolute value of the difference between the source term estimated by the inverse problem and the analytical source term given in equation (31). For the finer meshes, a stopping criterion of 5×10^{-2} was adopted. It can be observed that the number of iterations increases considerably from mesh 1 to 2. From mesh 2 to 3 this jump was even greater, reaching more than $17{,}000$ iterations. graphicx booktabs multirow

Table 1 – Simulation data for different mesh levels and degrees of disturbance in the experimental measurements.

Mesh	**No disturbance**			**1% disturbance**			**10% disturbance**		
	Time (s)	**Iterations**	N_∞	**Time (s)**	**Iterations**	N_∞	**Time (s)**	**Iterations**	N_∞
0	0.46	56	8×10^{-4}	1.29	100	9.63×10^{-4}	0.43	46	8.38×10^{-4}
1	4.72	230	9.18×10^{-4}	5.23	170	2.01×10^{-2}	5.80	184	9.86×10^{-4}
2	344.38	2718	8.83×10^{-4}	312.63	2368	9.84×10^{-4}	198.08	1190	9.96×10^{-4}

For the level 3 mesh, the optimization of f yields similar results when using either the analytical solution or data with a 1% disturbance as the experimental input. However, with a 10% disturbance, the obtained source term, Figure 15, was significantly amplified. This effect can be observed in Figure 14c. Another amplified effect was the number of iterations required for the inverse problem to converge, a similar behavior for the coarser meshes in which the stopping criterion was 10^{-4}.

Figures 6-14 present the graphs obtained with the solution of the inverse problem. Figure 5 presents the graphs representing the solution of the inverse problem on the sphere, source term, for the level 0 mesh, without disturbance, Figure 7(a), with 1% disturbance, Figure 7(b), and with 10% disturbance, Figure 7(c). Visually, it is not possible to observe any difference, however, observing Figure 7 it is clear that the perturbed solutions vary in proximity to the analytical solution. However, the solution without disturbance and with 1% disturbance practically overlap.

Figure 4 – Level 0 mesh: original and optimized source term.

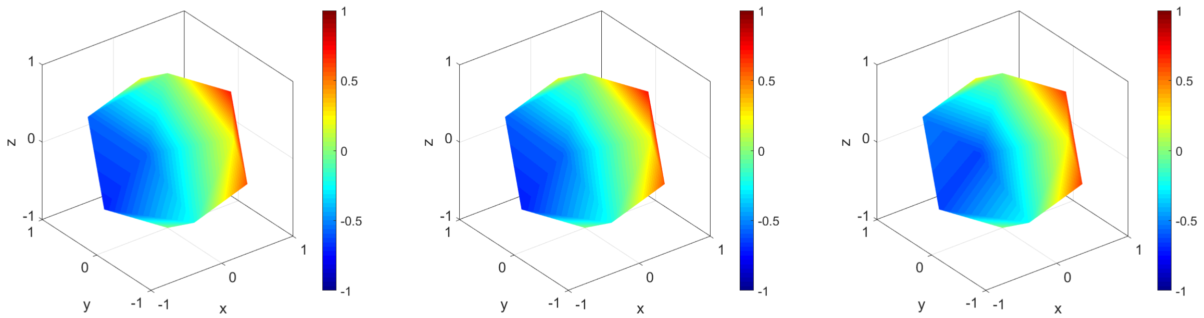

(a) without disturbance (b) disturbance 1% (c) disturbance 10%

Figure 5 – Level 0 mesh - $u[f]$ obtained.

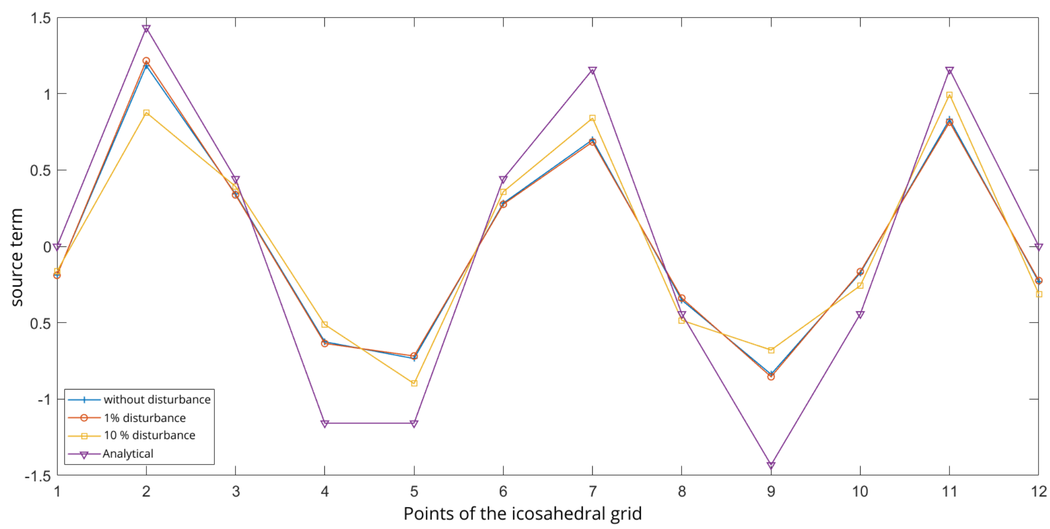

Figure 6 – Level 0 mesh - $u[f]$ obtained.

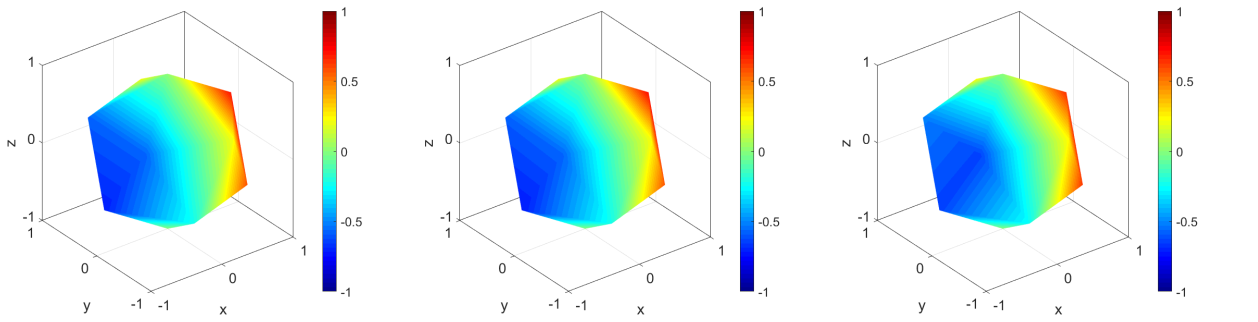

(a) without disturbance (b) disturbance 1% (c) disturbance 10%

Figure 7 – Level 0 mesh: original and optimized source term.

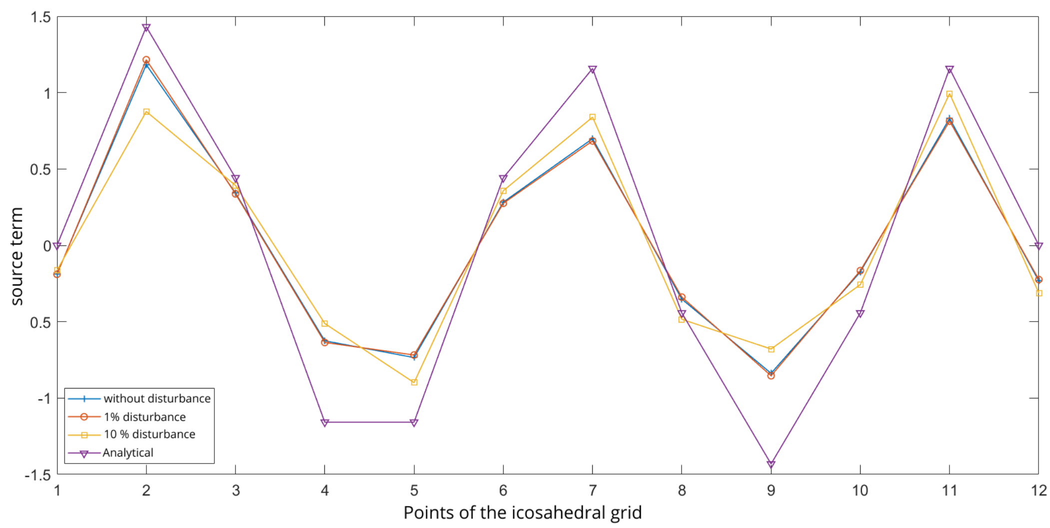

The solution of the inverse problem on the sphere in the level 1 mesh has the same behavior as the inverse problem in the level 0 mesh. The solutions without disturbance and with 1% disturbance practically overlap. It can be seen that all solutions recover the behavior of the source term, see Figure 10 and Figure 11.

Figure 8 – Level 1 mesh - $u[f]$ obtained.

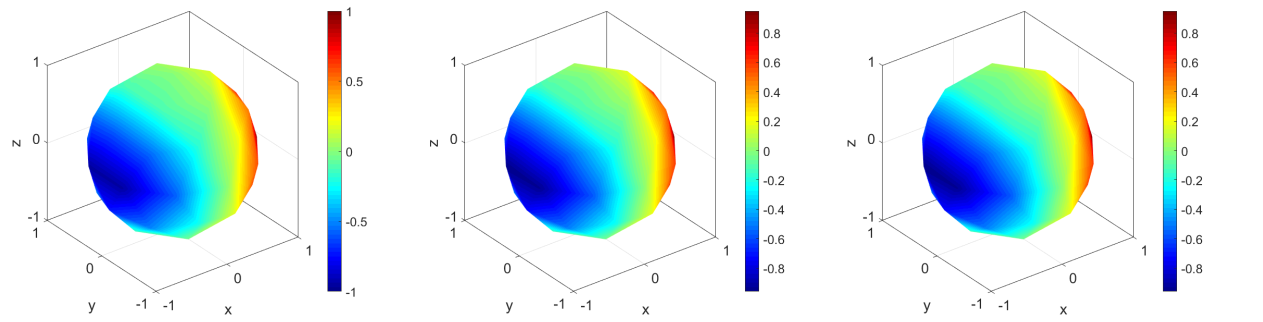

(a) without disturbance (b) disturbance 1% (c) disturbance 10%

Figure 9 – Level 1 mesh: original and optimized source term.

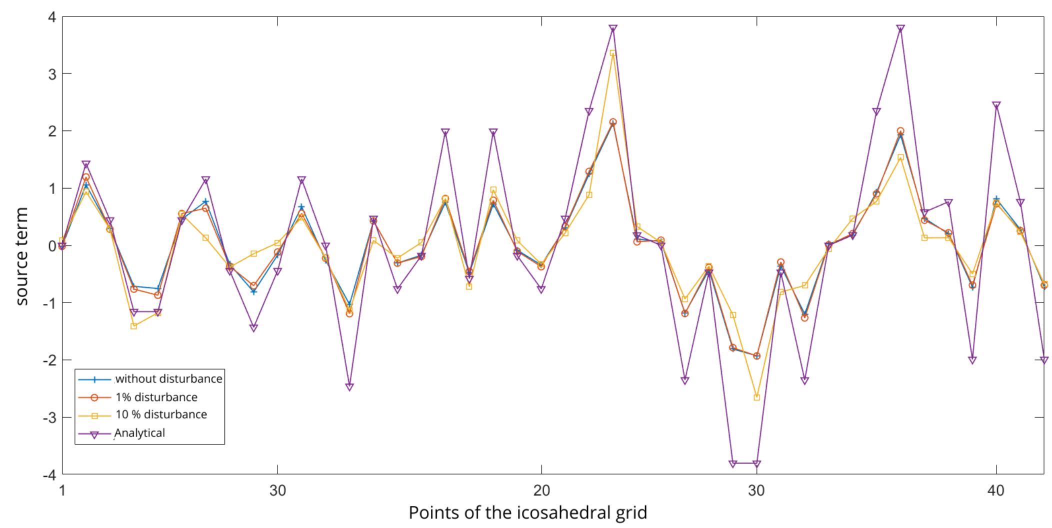

The solution of the inverse problem on the sphere in the level 1 mesh has the same behavior as the inverse problem in the level 0 mesh. The solutions without disturbance and with 1% disturbance practically overlap. It can be seen that all solutions recover the behavior of the source term, see Figure 10 and Figure 11.

Figure 10 – Level 1 mesh - $u[f]$ obtained.

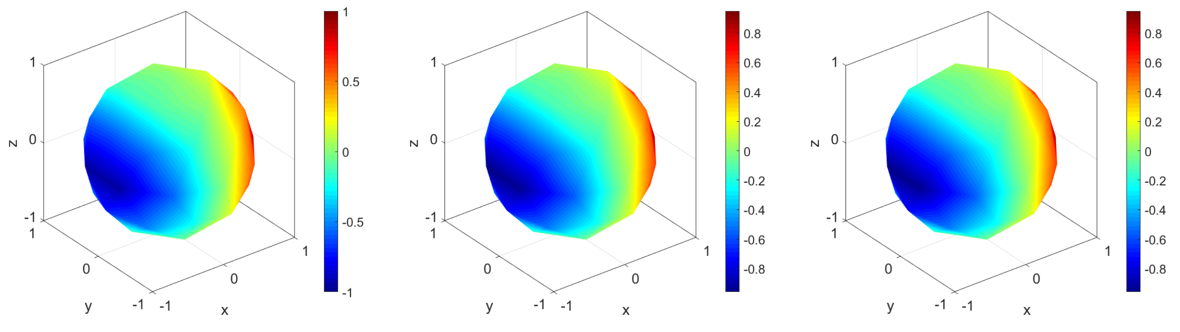

(a) without disturbance (b) disturbance 1% (c) disturbance 10%

Figure 11 – Level 1 mesh: original and optimized source term.

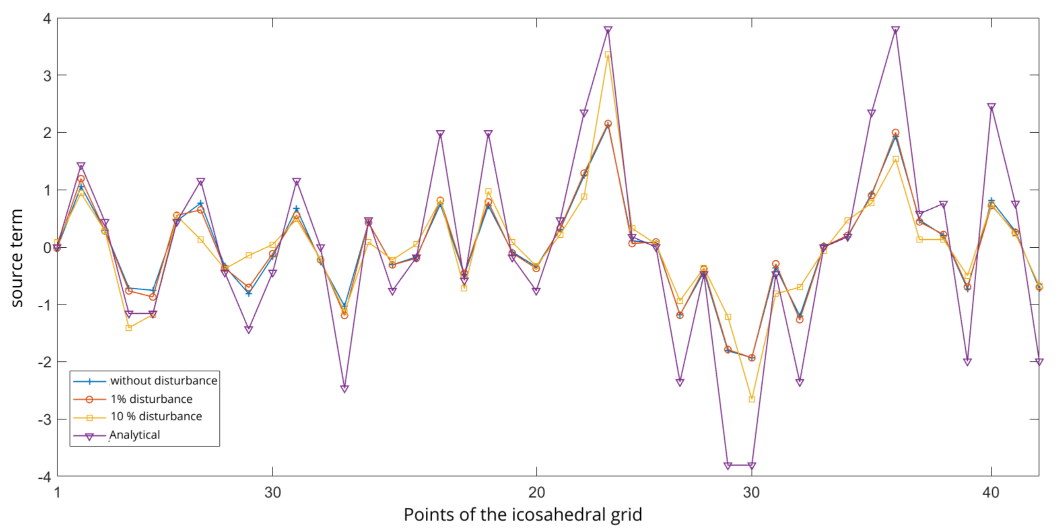

It can be observed that in the level 2 mesh there is already a difference in behavior in relation to the solution of the inverse problem in the previous meshes. The solutions without disturbance and with 1% of disturbance maintain the overlapping pattern, close to the original source term. However, the solution of the inverse problem with a disturbance of 10% in the experimental data begins to be amplified, and even recovering the same behavior of the source term, the amplification increases considerably at some points of the mesh. See Figure 12 and Figure 13.

Figure 12 – Level 2 mesh - $u[f]$ obtained.

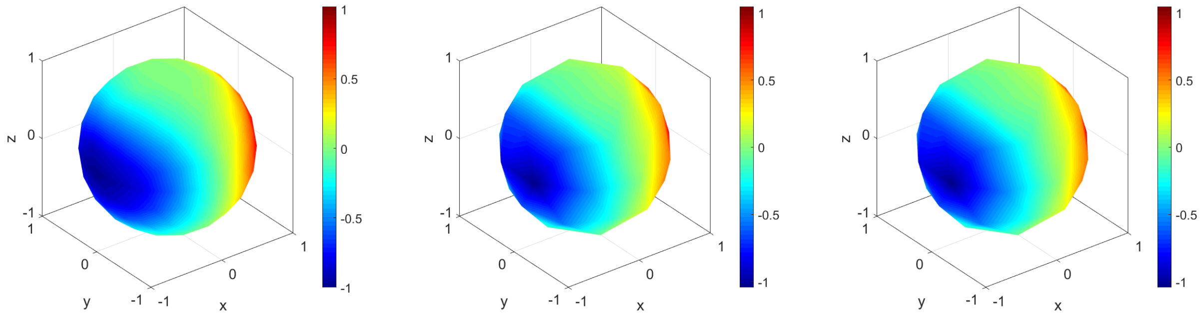

(a) without disturbance (b) disturbance 1% (c) disturbance 10%

Figure 13 – Level 2 mesh: original and optimized source term.

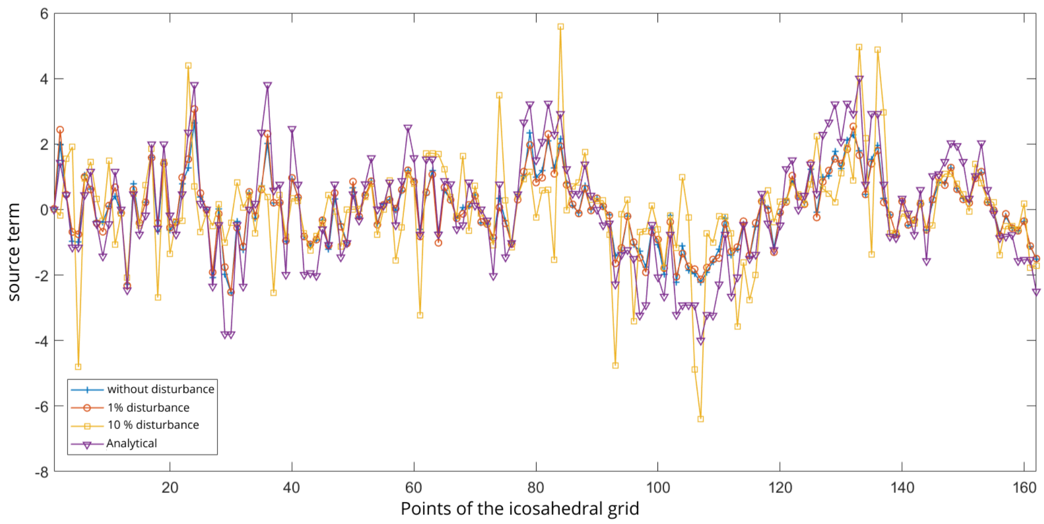

In Figure 15(c) the difference in the solution of the inverse problem is already visible. The source term recovered with 10% of disturbance in the experimental data, Figure 14, was greatly amplified. The solution recovers the same behavior of the source term. However, the solutions obtained with the experimental data without disturbance or with 1% of disturbance remain close to the source term, without major changes.

Figure 14 – Level 3 mesh - $u[f]$ obtained.

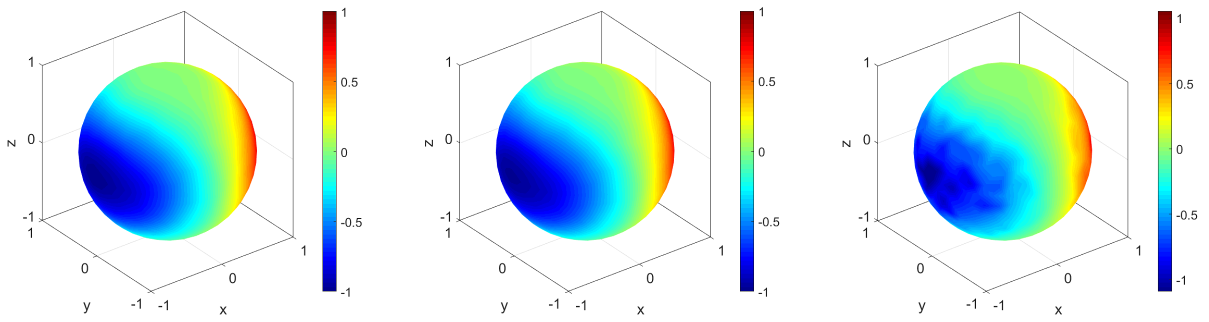

(a) without disturbance (b) disturbance 1% (c) disturbance 10%

Figure 15 – Level 3 mesh: original and optimized source term.

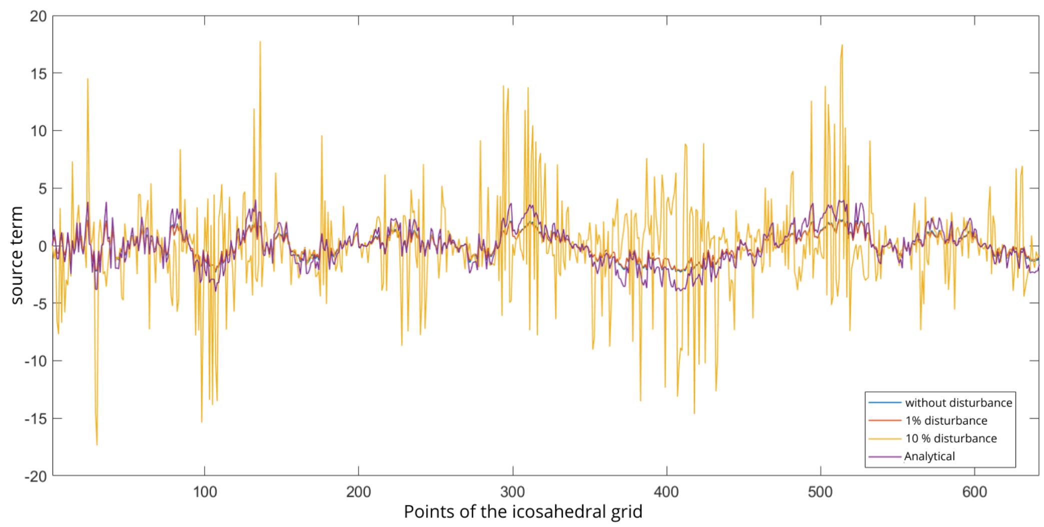

5 CONCLUSION

The results demonstrate the effectiveness of icosahedral spherical meshes for solving inverse problems associated with partial differential equations on spherical domains. The regularization method used recovered the source term for different levels of mesh refinement and degrees of disturbance in the experimental data. It was observed that, for mesh levels 0 and 1, the algorithm converges quickly, even with small disturbances in the data. As the mesh is refined, levels 2 and 3, the number of iterations and the computational time increase significantly, requiring more adjusted stopping criteria.

In addition, it was possible to observe that the solution of the inverse problem is sensitive to disturbances in the data. While disturbances of 1% produce solutions close to the analytical solution, a disturbance of 10% significantly amplifies the reconstructed source term, especially in the finer meshes. This behavior highlights the importance of a careful choice of the algorithm parameters.

In general, all solutions recovered the behavior of the source term. The exponential growth in the number of vertices in the icosahedral mesh leads to a considerable increase in algorithm execution time. It is important, in future work, to evaluate the parameters related to the mesh and discretization, both of the direct problem and the inverse problem.

REFERENCES

Alifanov, O. M. (1974). Solution of an inverse problem of heat conduction by iteration methods. *Journal of Engineering Physics*, 26:471–476.

Alifanov, O. M. & Mikhailov, V. V. (1978). Solution of the nonlinear inverse thermal conductivity problem by iteration method. *J. of Engineering Physics*, 35:1501–1506.

Augebaum, J. M. & Peskin, C. S. (1985). On the construction of the voronoi mesh on a sphere. *Journal of Computational Physics*, 59:177–192.

Baumgardner, J. R. & Friderickson, P. O. (1985). Icosahedral discretization of the two-sphere. *SIAM Journal on Numerical Analysis*, 22(6):1107–1115.

Chukkapalli, G., Karpik, S. R., & Ethier, C. R. (1999). A scheme for generating unstructured grids on spheres with application to parallel computation. *Journal of Computational Physics*, 149:114–127.

Douglas Jr., J., Paes Leme, P. J., Roberts, J. E., & Wang, J. (1993). A parallel iterative procedure applicable to the approximate solution of second order partial differential equations by mixed finite element methods. *Numerische Mathematik*, 65:95–108.

Ferreira, F. F. (2008). *Problemas Inversos sobre a Esfera*. Tese de doutorado, Instituto Politécnico - UERJ, Nova Friburgo, RJ.

Gonçalves, F. & Moura Neto, F. D. (2005). An iterative parallel algorithm for linear systems defined on graphs. *SIAM Journal on Numerical Analysis*.

Heikes, R. & Randall, D. A. (1995a). Numerical integration of the shallow-water equations on a twisted icosaedral grid. parte i: basic desing and results of tests. *Monthly Weather Review*, 123(6):1862–1880.

Heikes, R. & Randall, D. A. (1995b). Numerical integration of the shallow-water equations on a twisted icosaedral grid. parte ii: a detailed description of the grid and analysis of numerical accuracy. *Monthly Weather Review*, 123(6):1881–1887.

Karpik, S. R. & Peltier, W. R. (1991). Multigrid methods for the solution of poisson´s equation in a thick spherical shell. *SIAM Journal on Scientific and Statistical Computing*, 12(3):681–694.

Lanser, D., Blom, J. G., & Verwer, J. G. (2000). Spatial discretization of the shallow water equations in spherical geometry using osher's scheme. *Journal of Computational Physics*, 165(2):542–565.

Moura Neto, F. D. & Ferreira, F. F. (2006). Discretização da equação de poisson sobre a esfera. In *ANAIS do IX Encontro de Modelagem Computacional*.

Moura Neto, F. D. & Ferreira, F. F. (2007a). Solução numérica da equação de poisson sobre a esfera - parte i: formulação, existência e unicidade, e convergência do método iterativo. In *ANAIS do X Encontro de Modelagem Computacional*.

Moura Neto, F. D. & Ferreira, F. F. (2007b). Solução numérica da equação de poisson sobre a esfera - parte ii: resultados numéricos. In *ANAIS do X Encontro de Modelagem Computacional*.

Moura Neto, F. D. & Silva Neto, A. J. (2012). *An Introduction to Inverse Problems with Applications*. Springer Berlin, Heidelberg, 1nd edition.

Moura Neto, F. D., Su, J., & Silva Neto, A. J. (2002). Inverse problems for heat conduction: gradient methods and nonlinear models. *Applied Mathematical Modelling*, 26(8):1093–1111.

Nicholson, D. M. C. & Shelton, W. A. (2002). Removed sphere method for poisson's equation. *Journal of Physics: Condensed Matter*, 14(22):5601–5608.

Nicolaides, R. A. (1992). Direct discretization of planar div-curl problems. *SIAM Journal on Numerical Analysis*, 29(1):32–56.

Renka, R. J. (1984a). Algorithm 623: Interpolation on the surface of a sphere. *ACM Transactions on Mathematical Software*, 10(4):437–439.

Renka, R. J. (1984b). Algorithm 624: Triangulation and interpolation at arbitrarily distributed points in the plane. *ACM Transactions on Mathematical Software*, 10(4):440–442.

Renka, R. J. (1984c). Interpolation of data on the surface of a sphere. *ACM Transactions on Mathematical Software*, 10(4):417–436.

Renka, R. J. (1997). Algorithm 772: Stripack: Delaunay triangulation and voronoi diagram on the surface of a sphere. *ACM Transactions on Mathematical Software*, 23(3):416–434.

Sibson, R. (1978). Locally equiangular triangulations. *The Computer Journal*, 21(3):243–245.

Siewert, C. E. (1994). A radiative-transfer inverse-source problem for a sphere. *J. Quant. Spectrosc. Radiat. Transfer*, 52(2):157–160.

Sjöberg, L. E. (2012). Solutions to linear inverse problems on the sphere by tikhonov regularization, wiener filtering and spectral smoothing and combination - a comparison. *Journal of Geodetic Science*, 1(2):31–37.

Stuhne, G. R. & Peltier, W. R. (1996). Vortex erosion and amalgamation in a new model of large scale flow on the sphere. *Journal of Computational Physics*, 128:58–81.

Stuhne, G. R. & Peltier, W. R. (1999). New icosahedral grid-point discretizations of the shallow water equations on the sphere. *Journal of Computational Physics*, 148:23–58.

Teanby, N. A. (2006). An icosahedron-based method for even binning of globally distributed remote sensing data. *Computers & Geosciences*, 32:1442–1450.

Tomita, H., Satoh, M., & Goto, K. (2002). An optimization of the icosaedral grid modified by spring dynamics. *Journal of Computational Physics*, 183(1):307–331.

Tulovsky, V. & Papiz, L. (2001). Formula for the fundamental solution of the heat equation on the sphere. *Applied Mathematics Letters*, 14(7):881–884.

Wallis, C. G. R., W. Y. & McEwen, J. D. (2017). Sparse image reconstruction on the sphere: Analysis and synthesis. *IEEE Transactions on Image Processing*, 26(11):5176–5187.

Author contributions

1 – Fábio Freitas Ferreira
Mathematician
https://orcid.org/0000-0001-5878-7078 • fabiofreitasferreira@id.uff.br
Contribution: Conceptualization; Methodology; Writing – Original Draft Preparation

2 – Francisco Duarte Moura Neto
Mathematician
https://orcid.org/0000-0003-4944-9450 • fabiofreitasferreira@id.uff.br
Contribution: Literature Review, Writing – Review & Editing

How to cite this article

Ferreira, F. F., & Moura Neto, F. D. (2026). Alifanov's Iterative Regularization Method for the Poisson Source Term on Spherical Surfaces using Icosahedral Meshes. *Ciência e Natura*, Santa Maria, *v. 48,* e91903. DOI: https://doi.org/10.5902/2179460X91903.